

Siliceous–Clayey Rocks of the Jurassic Accretionary Prism, Khekhtsir Range, Sikhote Alin: Stratigraphy and Genesis

A. N. Filippov and I. V. Kemkin

Far East Geological Institute, Far East Division, Russian Academy of Sciences, Vladivostok, Russia

Received February 15, 2006

Abstract—Lithologic–stratigraphic aspects of siliceous–clayey rocks forming the Khabarovsk terrane of the Jurassic accretionary prism were studied in western spurs of the Bol'shoi Khekhtsir Range on the left side of the Ussuri River (Ussuri–Khekhtsir section). Two defined types of the examined section differ in the composition, age, and origin of their constituting rocks. The northern segment of the section is composed of middle Bajocian red–brown siliceous–tuffaceous silty and olive-gray silty mudstones that accumulated in the hemipelagic domain under the influence of continental provenance. Its southern segment is represented by lower Bathonian olive-gray siliceous mudstones, mudstones barren of any admixtures, and yellowish brown tuffaceous mudstones deposited far away from the continent in waters with abundant radiolarians. It is shown that these rocks are elements of two tectono-stratigraphic complexes that reflect different stages in the accretionary prism formation.

Key words: *Siliceous–clayey sediments, radiolarians, accretionary prism, Jurassic, Sikhote Alin.*

DOI: 10.1134/S181971400701006X

INTRODUCTION

The eastern margin of the Asian continent hosts widespread tectonic complexes or terranes of the Jurassic accretionary prism.¹ The prism formed over 70 m.y. during the subduction of the Paleo-Pacific (Panthalassa) oceanic plates and is of key importance for geodynamic reconstructions [6, 11, 12, 17, 24, 25, 30, 36, 44, 57, and others]. Its outcrops are traceable for over 5000 km from the left side of the Amur River lower reaches in the north via Sikhote Alin, the Japan and Ryukyu Islands, and the Island of Taiwan to Palawan Island (Philippines) in the south (Fig. 1a). The study of its structure, its subdivision into separate tectono-stratigraphic units, and their correlation in different terranes is of significance for reconstructing the successive formation of the accretionary prism and clarifying particularities of the accretion. In the opinion of some researchers, post-accretionary deformations substantially complicated the primary tectonic zonality of the prism and resulted in displacement of some of its fragments far away from the place of their formation [17, 30, 49]. Information on the age of the accreted paleoceanic fragments constituting the Jurassic accretionary prism and their composition and structure, which makes it possible to subdivide it into tectono-stratigraphic units, is obtained in sufficient quantity

only for its central (southern Sikhote Alin, Japan) and southern (Ryukyu Island, Philippines) parts [9, 10, 47, 57], while its northern segment comprising the Nadan'khada Alin, Khabarovsk, and Badzhal terranes is insufficiently studied in this respect.

The accretionary prisms are usually characterized by a wide distribution of the nappe–thrust dislocations, melange, ophiolites, and packets of tectonic sheets with fragments of sedimentary cover blanketing the oceanic plate. The latter forms a certain succession, the so-called “oceanic plate stratigraphy” [29], representing an important feature of ancient accretionary prisms [33, 39, 40, 56]. In the Jurassic accretionary prism, it is usually composed (from the base upward) of pelagic cherts, hemipelagic sediments, terrigenous siltstones, and sandstones formed in the near-continent sedimentation settings. It is believed that such a vertical succession reflects sedimentation on the oceanic crust from the moment of its origination within the spreading ridge to its burial in the subduction zone. In this succession, most informative are hemipelagic sediments represented usually by siliceous mudstones, mudstones, and silty mudstones. They frequently contain well-preserved radiolarians, whose age marks the arrival time of particular oceanic plate segments to the convergence zone. In addition, the composition of the hemipelagic sediments provides information on the sedimentation and tectonic settings in the convergence zone. For example, it helped to define different-age tectono-stratigraphic units in some fragments of the Jurassic

¹ The “Jurassic” accretionary prism is named conditionally for the sake of brevity, since its formation in some areas of the continental margin commenced in the terminal Triassic [34] and terminated in the Berriasian or, probably, Valanginian of the Early Cretaceous [22, 41, 54]

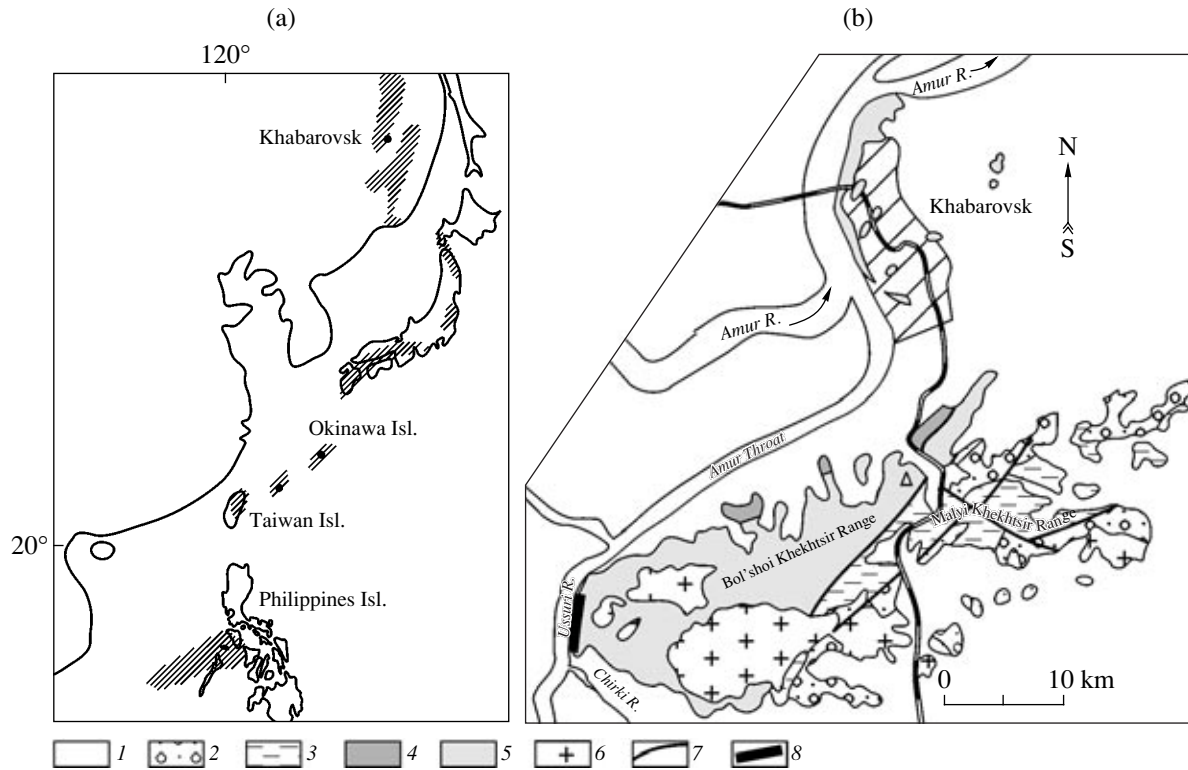


Fig. 1. (a) Fragments of the Jurassic accretionary prism (shaded) in eastern Asia, after [36, 40, 57]; (b) Schematic geological map of the Khabarovsk area and Bol'shoi and Malyi Khekhtsir ranges, after [14].

(1) Quaternary sediments; (2, 3) terrigenous sediments: (2) Aptian–Albian, (3) Berriasian(?)–Valanginian; (4, 5) volcanogenic–siliceous–terrigenous rocks of the accretionary complex: (4) Permian, (5) Triassic–Jurassic; (6) granite; (7) faults; (8) examined section along the Ussuri River downstream of the Chirka River mouth.

accretionary prism and to reconstruct its structure and formation history [9, 10, 47, 57].

This paper presents the results of paleontological and lithologic–stratigraphic studies of siliceous–clayey sediments in western spurs of the Bol'shoi Khekhtsir Range on the left side of the Ussuri River. They allow us to distinguish two rock types differing in their composition, age, and origin. These rocks represent elements of tectono-stratigraphic complexes that reflect different stages in the formation of the Khabarovsk segment of the Jurassic accretionary prism.

REGIONAL TECTONICS AND PREVIOUS STUDIES

Khanchuk [23, 24] and Kemkin [11] attribute the study area (Khekhtsir Range) to the Khabarovsk terrane, which extends as a band 100–130 km wide northeastward from the Naolikh River valley in the south via the Khekhtsir Range and Khabarovsk Heights to the Vandan, Gorbylyak, and Sagdayan ranges in the north. Zيابrev [8, 58] considers it as the southeastern youngest part of the Badzhal terrane of the Jurassic accretionary complex. Natal'in [1, 17, 53] regards the Badzhal terrane as an autonomous structure that differs from the Jurassic accretionary complexes of Sikhote Alin and

includes the study area into the Early Cretaceous Khabarovsk accretionary complex of the Khingan–Okhotsk active continental margin. The recent data indicate, however, the Jurassic age of the Khabarovsk complex [32, 58], and the similarity of its composition and structure with the Samarka terrane substantiates the standpoint that the former represents a fragment of the northern flank of a single Jurassic accretionary prism [11, 33, 58].

Volcano-sedimentary rocks of the Khekhtsir Range were previously referred to the Upper Triassic–Lower Jurassic Krasnaya Rechka Formation. Structurally, it was considered as multiply repeated beds of siliceous, terrigenous, and basic volcanic rocks and their age was first based on fossils in limestones from the Mount Dva Brata locality [5, 18]. Subsequently, based on finds of Early Permian and Triassic conodonts and Triassic and Early Jurassic radiolarians, these rocks have been subdivided into the Triassic–Jurassic siliceous and Jurassic–Lower Cretaceous sequences, the latter composed of mixtites, siltstones, sandstones, and basic volcanics with allochthonous sheets of Permian rocks [3, 13, 27]. Zيابrev [8], who studied these rocks in steeps of the Ussuri River right bank, defined tectonic sheets 10 to 100 m thick separated by melange zones and composed of siliceous, siliceous–clayey, and clastic rocks with

subordinate basalts. The primary succession of beds reconstructed by the last author using relationships between different lithological elements is the following (from the base upward): (1) bedded cherts (up to 100 m); (2) red-brown siliceous aleuropelites (approximately 10 m); (3) olive-gray siliceous aleuropelites (not more than 100 m); (4) clastic rocks (not more than 100 m). Although the age of the rocks remained undetermined, they were correlated with similar succession of the neighboring Khabarovsk complex, where the stratigraphic position of different members was substantiated by radiolarian and conodont finds [2, 3, 7, 13, 16, 27, 35, 55]. We established the age of siliceous-clayey rocks from this section and specified their composition, which allowed us to correct the stratigraphy and structural interpretations for the area under consideration.

EXAMINED OBJECTS AND METHODS

Siliceous-clayey interbeds and their host rocks outcropping in steeps along the right Ussuri River bank downstream of the Chirka River (Ussuri-Khekhtsir section) served as the object for this study (Fig. 1b). The attitude and textural-structural features of the rocks were studied in outcrops and in polished samples. For age determination, samples were collected for the radiolarian analysis. Radiolarians were extracted using a weak solution of hydrofluoric acid, then picked from the residue and studied under a scanning electron microscope. The rock composition was determined in thin sections under a polarizing microscope. The samples were subjected to a chemical analysis and an analysis of heavy minerals. Oxides for the bulk chemical composition were determined using weight analysis. Heavy minerals were extracted by bromoform from samples of 0.2–1.0 kg crushed to the fraction of 0.25 mm (the fraction of <0.01 mm was removed). Their composition was determined using immersion liquids under a microscope in transmitted and polarized light. The chemical composition of some heavy minerals was measured using a JXA-8100 microprobe at the Far East Geological Institute, Far East Division, Russian Academy of Sciences.

STRATIGRAPHY OF SILICEOUS-CLAYEY SEQUENCES

Siliceous-clayey rocks are largely developed in the **southern** and **northern** parts of the Ussuri-Khekhtsir section outcrop (Fig. 2).

The **southern segment** is represented by tectonic sheets of variable thickness composed of siliceous to clayey rocks and melange with large lenses of cherts and sandstones enclosed in an aleuropelitic matrix. They form a homocline turned over at steep angles northwestward (Fig. 2b). The following succession is reconstructed using attitude elements and radiolarian dates (Fig. 3; from the base upward):

(1) Greenish gray cherts and subordinate red-brown red-brown cherts, thin platy (1–3 cm), recrystallized, with an unclear relationship with the overlying rocks; the thickness is 30 m;

(2) Red-brown red-brown cherts, clayey, platy; the contact with the overlying rocks is tectonic; the thickness is 2 m;

(3) Greenish gray cherts, clayey, thin to medium platy (2–5 cm), with interbeds of olive-gray siliceous argillite (up to 2–3 cm); the upper part of the member (1 m) is composed of alternating clayey cherts (2–5 cm) and siliceous argillite (3–7 cm); the thickness is 4 m;

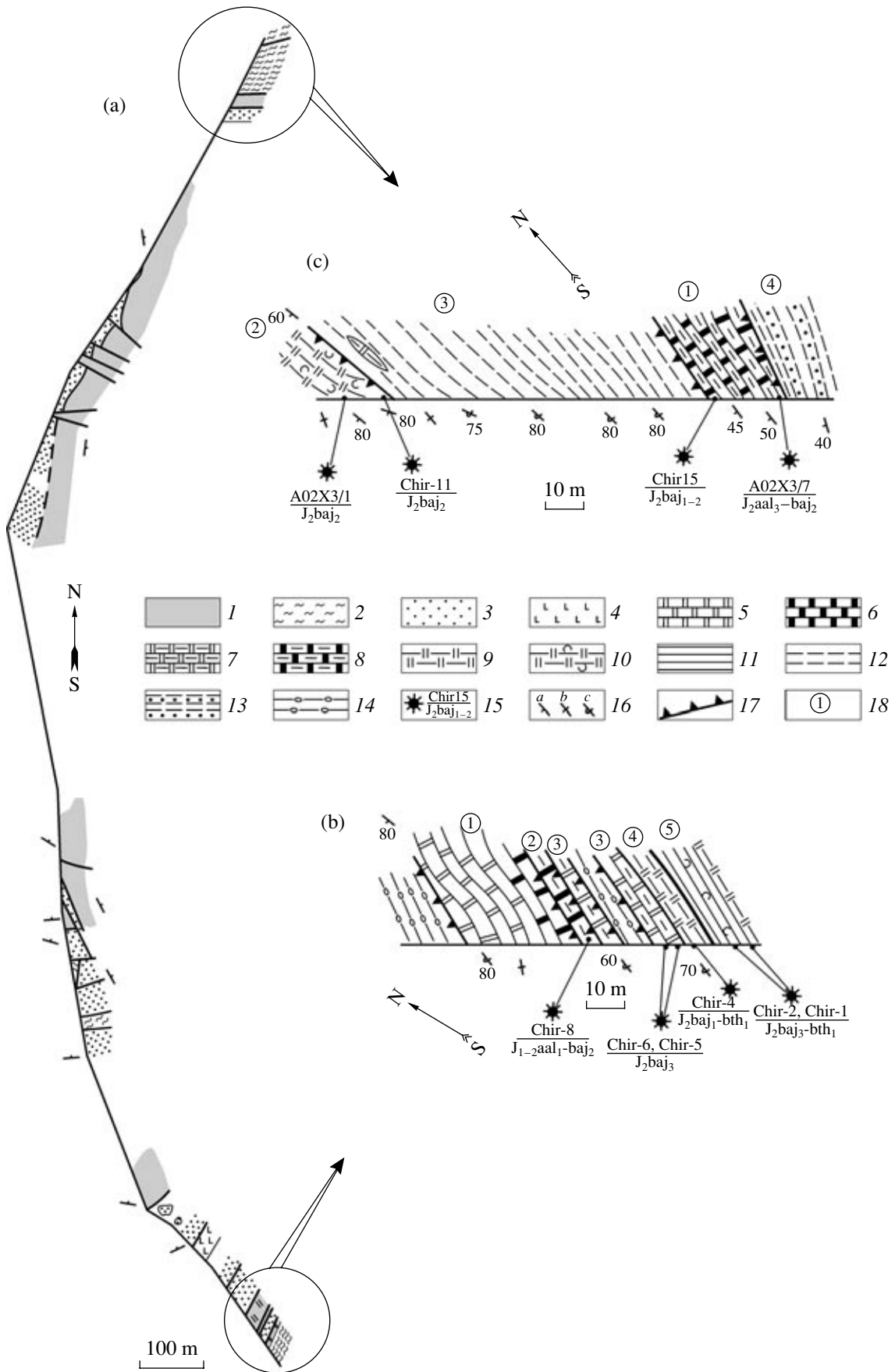
(4) Olive-gray siliceous massive argillite; the thickness is 5 m;

(5) Olive-gray bedded argillite grading into siliceous argillite in the upper 3 m and enclosing an interbed of yellowish brown tuffaceous argillite (2 m) in the middle part; the thickness is 14 m.

Members 2–5 yielded radiolarians (Table 1; Plate 1). Clayey red-brown cherts of Member 2 contain an early Aalenian–middle Bajocian radiolarian assemblage (sample Chir-8). The lower and upper age limits correspond to the first occurrence (FO) level of *Parahsuum officerence* and the last occurrence (LO) level of *Parahsuum grande*, respectively [28]. Clayey cherts of Member 3 enclose late Bajocian radiolarians (samples Chir-5 and Chir-6). Such an age is confirmed by co-occurring *Triactoma blakei*, *Tricolocapsa conexa*, *T. multispinosa*, and *Protunuma turbo* with the FO in the late Bajocian and *Yamatoum spinosum*, *Unuma typicus*, *Eucyrtidellum quinatum*, and *Archicapsa pachyderma*, which became extinct in the late Bajocian [28, 42, 43, 51, 52]. The FO of *Tricolocapsa conexa* is recorded in the terminal early Bathonian [43, 51]. The joint find of the last species with the above-mentioned taxa indicates, however, its older age. Siliceous argillite from Member 4 (sample Chir-4) yields the radiolarians *Stichocapsa japonica*, *Dictyomitrella kamoensis*, and *Tricolocapsa fusiformis*, whose co-occurrence characterizes the early Bajocian–early Bathonian interval [28, 43, 51]. Inasmuch as the underlying clayey cherts are of the late Bajocian in age, the siliceous argillite is most likely

Fig. 2. Structure of the accretionary complex in the Ussuri-Khekhtsir section (a) and its thoroughly studied southern (b) and northern (c) segments (after [8]).

(1–13) rocks: (1) siliceous, (2) siliceous-clayey, (3) detrital varieties and melange, (4) basalt, (5) chert, (6) red-brown chert, (7) clayey chert, (8) clayey red-brown cherts, (9) siliceous argillite, (10) siliceous-tuffaceous silty argillite, (11) argillite, (12) silty argillite, (13) silty argillite with sandstone interbeds; (14) melange; (15) radiolarian finds, sample numbers, and age indices; (16) attitude: (a) normal, (b) vertical, (c) overturned; (17) faults; (18) bed number.



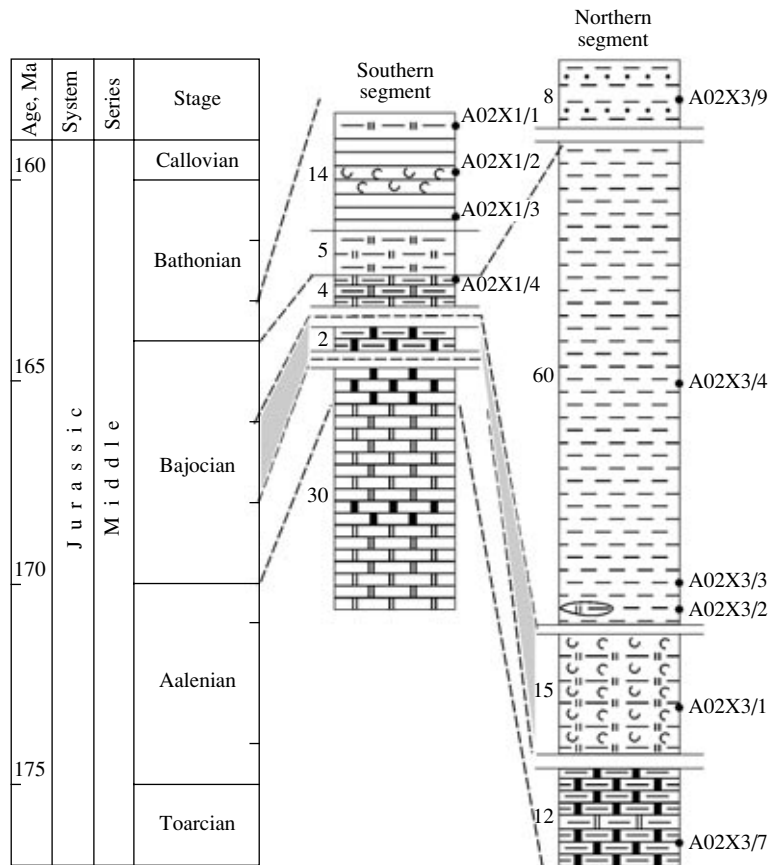


Fig. 3. Correlation of siliceous-clayey sediments in the southern and northern segments of the Ussuri-Khekhtsir section.

The numerals to the left and right of the columns designate the thicknesses of members and the numbers of samples collected for analyses, respectively. The geochronologic and stratigraphic scales are after [28]. For the legend, see Fig. 2.

correlative with the early Bathonian (sample Chir-4 is located 1.5 m above sample Chir-5). Bedded argillite of Member 5 provided late Bajocian-early Bathonian radiolarians (samples Chir-1 and Chir-2). The lower age limit of this assemblage corresponds to the FOs of *Stylocapsa testa*, *Tricolocapsa multispinosa*, *T. conexa*, and *Protunuma turbo* [28, 42, 52], while its upper limit is determined by the presence of *Tricolocapsa plicarum* and *T. fusiformis*, which became extinct in the early Bathonian [28, 42, 43]. The FO of *Stylocapsa testa* is registered in the late Bathonian [43, 51]. If this is the case, the species in question cannot occur together with *Tricolocapsa plicarum* and *T. fusiformis* and its range should be accepted after [28, 42]. Thus, the age of the argillite from Member 5 corresponds to the early Bathonian.

The northern segment is formed by tectonic sheets consisting of siliceous, clayey, and detrital rocks dipping northwestward at angles of 45°–80° (Fig. 2c). The sheet composed of silty argillite is probably overturned. The stratigraphic succession is the following (Fig. 3; from the base upward):

(1) Brown red-brown cherts, clayey, bedded, obscurely thin platy, with greenish gray clayey cherts in the middle part of the member; the relationships with the overlying rocks are unclear; the thickness is 12 m.

(2) Red-brown tuffaceous siltstones, siliceous, massive, with lenses of clayey cherts and red-brown cherts (up to 7 cm thick) at the base; the upper boundary is tectonic; the thickness is 15 m;

(3) Olive-gray massive silty argillite with interbeds (up to 5 cm) of brown and red-brown siliceous-clayey rocks at the base; the thickness is 60 m;

(4) Dark greenish gray silty argillite with interbeds (5–40 cm) of gray inequigranular sandstones; the relationship with underlying rocks is unclear; the thickness is 8 m.

Members 1 and 2 contain radiolarians (Table 1; Plate 2). The clayey red-brown cherts of Member 1 (samples A02X3/7 and Chir-15) yield a radiolarian assemblage of a wide stratigraphic range. The terminal Aalenian-middle Bajocian age of red-brown cherts from the member base (sample A02X3/7) was determined based on the find of *Parahsuum hiconocosta* and *Laxtorum(?) jurassicum*. The lower and upper age lim-

Table 1. Radiolarians from siliceous and clayey rocks of the Ussuri–Khekhtsir section

Radiolarians	Samples											
	Chir-1	Chir-2	Chir-4	Chir-5	Chir-6	Chir-8	Chir-10	Chir-11	Chir-15	A02X3/1	A02X3/7	
<i>Archaeodictyomitra elliptica</i> Vishnevskaya	cf.				+							
<i>Archaeodictyomitra exigua</i> Blome	+	+		+	+		cf.	cf.		cf.		
<i>Archicapsa pachyderma</i> Tan Sin Hok	cf.	cf.		cf.	cf.		cf.	cf.	cf.	+	cf.	
<i>Dictyomitrella kamoensis</i> Mizutani et Kido	+	+	+	+	+		+	+	+	+		
<i>Emiluvia premyogii</i> Baumgartner				cf.								
<i>Eucyrtidiellum nodosum</i> Wakita					+							
<i>Eucyrtidielum ptictum</i> (Riedel et Sanfilippo)				+								
<i>Eucyrtidiellum quinquatum</i> Takemura				+				cf.				+
<i>Eucyrtidiellum unumaense</i> Yao	+	+		+	+							
<i>Hsuum belliatulum</i> Pessagno et Whalen		+						+				
<i>Hsuum matsukokai</i> Isozaki et Matsuda								cf.				+
<i>Hsuum parasolense</i> Pessagno et Whalen								+		+		+
<i>Laxtorum(?) jurassicum</i> Isozaki et Matsuda 1								+				+
<i>Parahsuum hiconocosta</i> Baumgartner et Dewever												+
<i>Parahsuum grande</i> Hori et Yao							+					+
<i>Parahsuum izeense</i> (Pessagno et Whalen)								+		+		+
<i>Parahsuum levicostatum</i> Takemura												+
<i>Parahsuum officerence</i> (Pessagno et Whalen)	cf.					cf.	cf.	+				+
<i>Parvicingula dhimenaensis</i> s.l. Baumgartner		cf.		+			+	+		+		+
<i>Parvicingula nanoconica</i> Hori et Otsuka												+
<i>Parvicingula omgoniensis</i> Vishnevskaya								+				
<i>Protunuma fusiformis</i> Ichikawa et Yao	+			+	+		+			+		
<i>Protunuma turbo</i> Matsuoka		+		cf.	+		+					
<i>Sethocapsa funatoensis</i> Aita		+		+								
<i>Stichocapsa convexa</i> Yao	+			cf.				+		+		
<i>Stichocapsa cribata</i> Hinde	+			+								
<i>Stichocapsa japonica</i> Yao	+	+	+	+	+		+	+		+		
<i>Stichomitra mediocris</i> (Tan)		+		+								
<i>Stylocapsa testa</i> Matsuoka	cf.											
<i>Transhsuum brevicostatum</i> (Ozoldova)	+	+		+	+		+	+		+		
<i>Transhsuum hisuikyoense</i> (Isozaki et Matsuda)												+
<i>Transhsuum maxwelli</i> (Pessagno)	+	+		+	+		+	+		+		
<i>Transhsuum medium</i> Takemura							+					
<i>Triactoma blakei</i> (Pessagno)				cf.								
<i>Tricolocapsa conexa</i> Matsuoka	aff.	+		aff.								
<i>Tricolocapsa fusiformis</i> Yao	+	+	cf.	+	cf.		+	cf.				
<i>Tricolocapsa multispinosa</i> Sashida	+			cf.								
<i>Tricolocapsa plicanum</i> Yao	+			+	+							
<i>Unumu ecliiatus</i> Iclukau a ct Yao	cf.			cf.								
<i>Unuma typicus</i> Ichikawa et Yao				+						+		
<i>Yaniatoitni spinosum</i> Takemura		+		cf.								

Table 2. Chemical composition of Middle Jurassic sedimentary rocks in the Ussuri–Khekhtsir section

Sample	Rock	Age	SiO ₂	TiO ₂	Al ₂ O ₃	Fe ₂ O ₃	FeO	MnO	MgO	CaO	Na ₂ O	K ₂ O	H ₂ O ⁻	P ₂ O ₅	L.O.I.	Sum
A02X1/1	Siliceous argillite	J ₂ bt ₁	76.49	0.48	10.95	3.42	0.40	0.12	1.31	0.23	1.30	1.94	0.30	0.08	2.67	99.69
A02X1/2	Tuffaceous argillite	J ₂ bt ₁	62.48	0.68	16.91	6.35	0.89	0.22	1.24	0.44	2.05	3.35	0.81	0.16	4.16	99.74
A02X1/3	Argillite	J ₂ bt ₁	64.16	0.60	13.88	5.88	0.73	0.32	1.55	1.90	1.79	2.85	0.9	0.87	4.11	99.62
A02X1/4	Clayey chert	J ₂ bj ₃	79.37	0.48	9.25	3.28	0.20	0.14	0.89	0.31	1.13	2.52	0.23	0.20	1.94	99.94
A02X3/1	Siliceous–tuffaceous silty argillite	J ₂ bj ₂	71.00	0.49	13.35	4.60	0.62	0.23	0.79	0.28	2.44	2.71	0.33	0.06	2.60	99.5
A02X3/2	Silty argillite	J ₂ bj ₃	60.90	0.85	16.45	6.25	0.68	0.12	1.70	1.03	2.63	2.56	1.53	0.15	4.70	99.55
A02X3/3	Silty argillite	J ₂ bj ₃	61.15	0.93	16.20	5.75	1.16	0.15	1.69	1.11	2.63	2.71	1.51	0.15	4.44	99.58
A02X3/4	Silty argillite	J ₂ bj ₃	61.95	0.97	15.70	5.20	1.40	0.13	2.00	1.10	2.78	2.65	0.79	0.14	4.78	99.59
A02X3/7	Clayey red-brown cherts	J ₂ aal ₂ –bj ₂	76.64	0.39	10.18	3.30	1.04	0.19	0.75	0.31	1.28	2.69	0.29	0.05	2.46	99.57
A02X3/9	Sandstone	J ₂ bt ₁ ?	70.31	0.52	14.75	3.05	0.56	0.19	0.85	0.76	3.56	2.05	0.42	0.10	2.78	99.90

Note: The rocks were analyzed at the Far East Geological Institute, Far East Division, Russian Academy of Sciences by the weight chemical method. The analysts were S.P. Batalova and G.I. Makarova.

its correspond to the FO levels of the former [28] and last [28, 43] species, respectively. The clayey red-brown cherts of the uppermost part of the member (sample Chir-15) are dated back to the early–middle Bajocian. Their lower age limit corresponds to the FO of *Dictyomitrella kamoensis* [28], while the upper one is derived from the position of red-brown siliceous–tuffaceous silty argillite overlying brown red-brown cherts (see below). Siliceous–tuffaceous silty mudstones of Member 2 (samples Chir-10, Chir-11, A02X3/1) provided the radiolarians *Hsuum belliatulum*, *Stichocapsa japonica*, and *Parahsuum izeense*, whose co-occurrence indicates the middle Bajocian age of the host

rocks [28]. The silty mudstone from Member 3 overlying siliceous–tuffaceous silty argillite is probably of the late Bajocian in age.

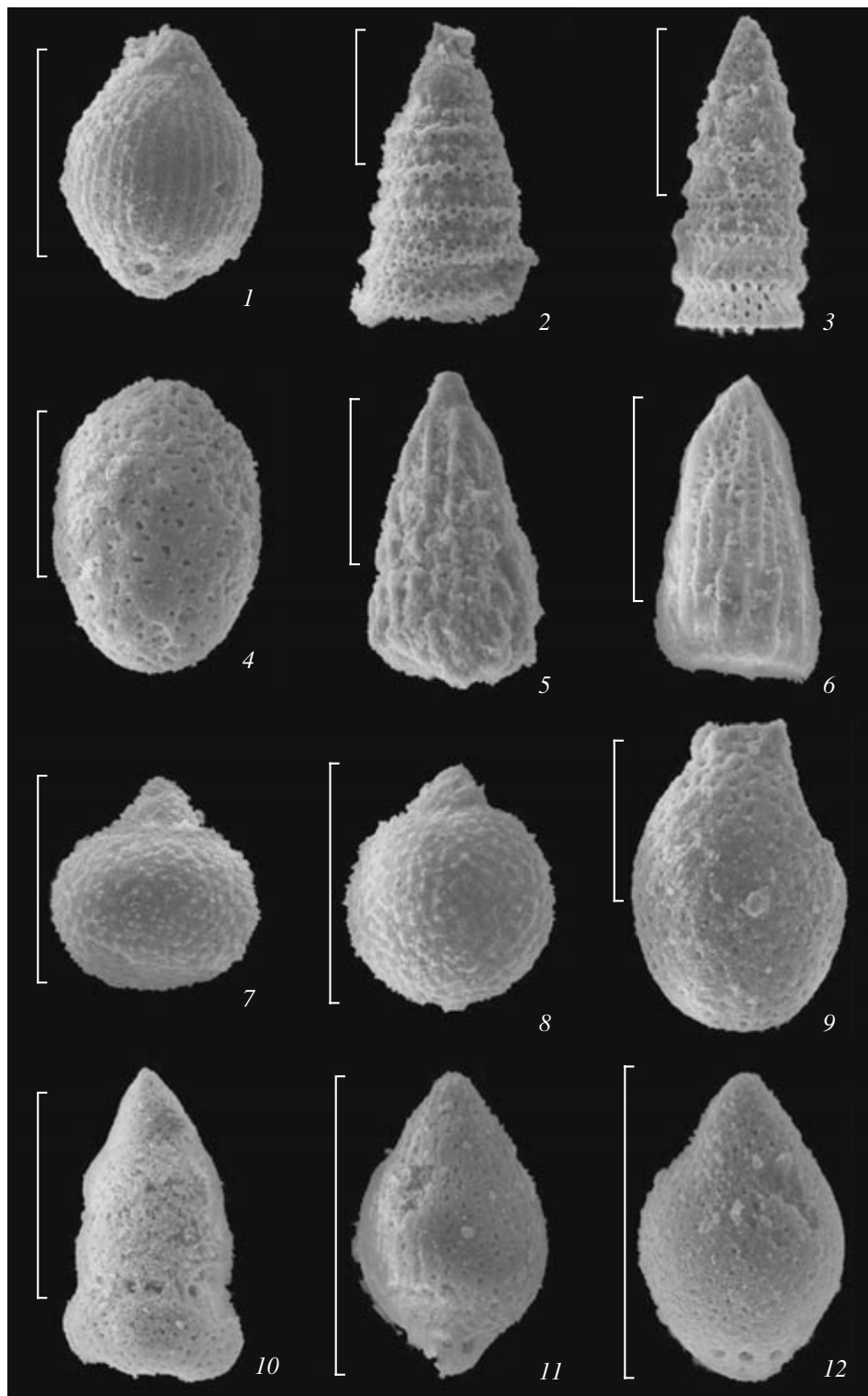
Small tectonic blocks in the central part of the section enclose red-brown siliceous–tuffaceous silty mudstones (Fig. 2a) similar to those constituting Member 2 in the northern segment. The radiolarian assemblage extracted from these rocks is similar to its counterpart from samples Chir-11 and A02X3/1.

Thus, the siliceous–clayey rocks of the Ussuri–Khekhtsir section characterize two different successions (Fig. 3). In the southern part of the section, clayey cherts grade first to olive-gray siliceous argillite and,

Plate 1. Late Bajocian–early Bathonian radiolarians from siliceous–clayey rocks of the Ussuri–Khekhtsir section southern segment. The bar length is 100 mm.

(1) *Tricolocapsa plicarum* Yao, sample Chir-1; (2, 3) *Dictyomitrella kamoensis* Mizutani et Kido: (2) sample Chir-1, (3) sample Chir-2; (4) *Archicapsa* cf. *pachyderma* Tan Sin Hok, sample Chir-1; (5, 6) *Transhuum maxwelli* (Pessagno); (5) sample Chir-1, (6) sample Chir-5; (7, 8) *Tricolocapsa multispinosa* Sashida, sample Chir-1; (9) *Stylocapsa* cf. *testa* Matsuoka, sample Chir-1; (10) *Stichocapsa japonica* Yao, sample Chir-5; (11, 12) *Tricolocapsa fusiformis* Yao: (11) sample Chir-5, (12) sample Chir-6; (13, 14) *Protunuma fusiformis* Ichikawa et Yao: (13) sample Chir-5, (14) sample Chir-6; (15) *Parvicingula dhimenaensis* s.l. Baumgartner, sample Chir-10; (16) *Eucyrtidiellum unumaense* Yao, sample Chir-1; (17) *Transhuum brevicostatum* (Ozoldova), sample Chir-5; (18) *Emiluvia* cf. *premyogii* Baumgartner, sample Chir-5; (19) *Eucyrtidiellum quinquatum* Takemura, sample Chir-5; (20, 21) *Tricolocapsa conexa* Matsuoka, sample Chir-2; (22) *Protunuma turbo* Matsuoka, sample Chir-2; (23) *Yamatoum spinosum* Takemura, sample Chir-2; (24) *Sethocapsa funatoensis* Aita, sample Chir-2.

Plate 1



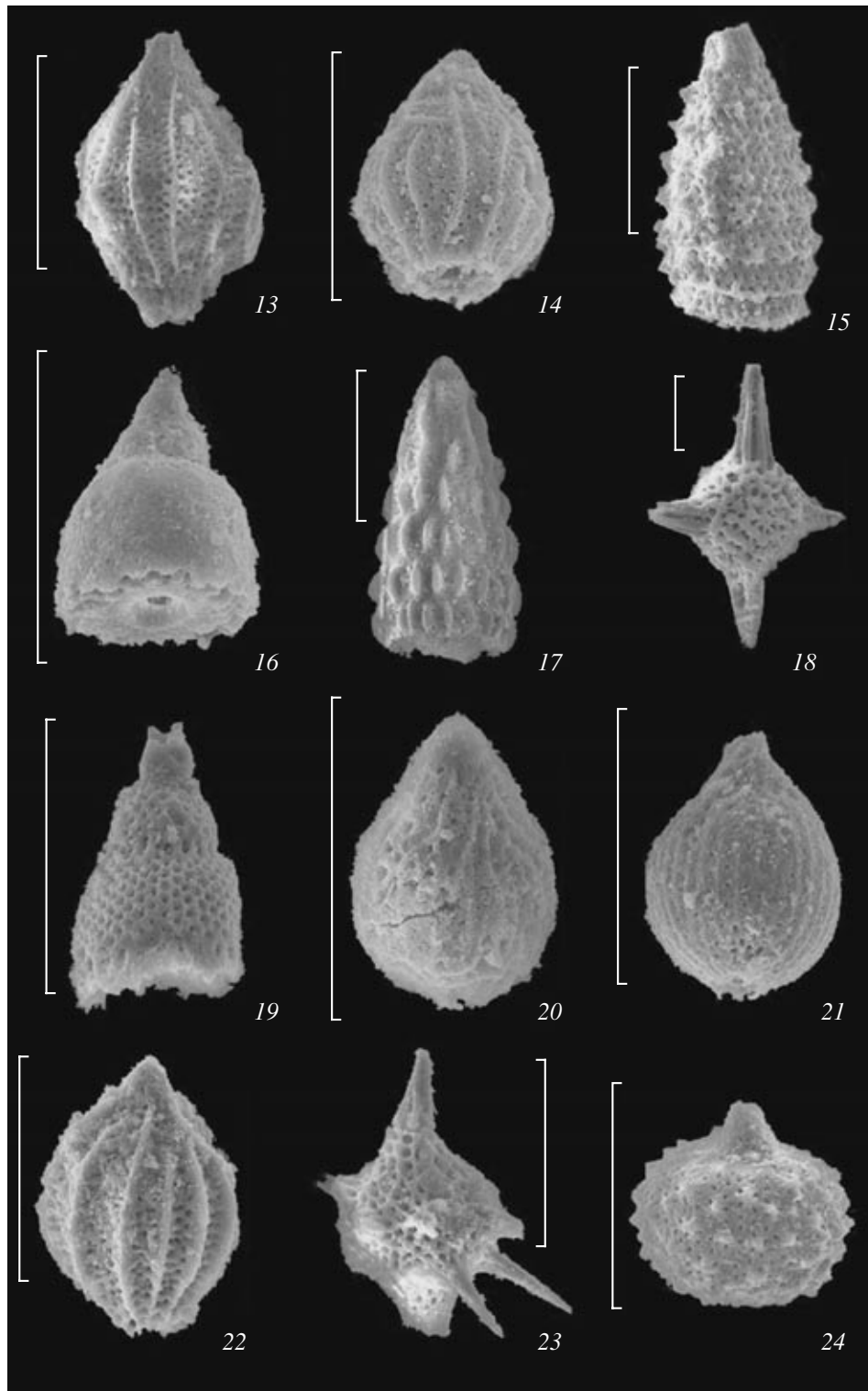


Plate 2. Aalenian–early Bajocian radiolarians from siliceous–clayey rocks of the Ussuri–Khekhtsir section northern segment. The bar length is 100 mm.

(1–4) *Parahsuum grande* Hori et Yao: (1, 2) sample A02X3/7, (3, 4) sample Chir-8; (5, 6) *Laxtorum(?) jurassicum* Isozaki et Matsuda: (5) sample Chir-11, (6) sample A02X3/7; (7) *Hsuum* cf. *parasolense* Pessagno et Whalen, sample Chir-11; (8) *Hsuum* cf. *beliatulum* Pessagno et Whalen, sample Chir-11; (9) *Paronaella* sp., sample Chir-11; (10) *Stichocapsa conexa* Yao, sample Chir-11; (11) *Unuma typicus* Ichikawa et Yao, sample A02X3/1; (12) *Parahsuum officerence* (Pessagno et Whalen), sample A02X3/7; (13, 14) *Transhsuum* cf. *hisuikyoenae* (Isozaki et Matsuda), sample A02X3/7; (15) *Eucyrtidiellum* cf. *quinatum* Takemura, sample A02X3/7; (16) *Parahsuum levicostatum* Takemura, sample A02X3/7; (17) *Hsuum matsukai* Isozaki et Matsuda, sample A02X3/7; (18) *Parahsuum* sp., sample A02X3/7; (19) *Parvicingula nanoconica* Hori et Otsuka, sample A02X3/7; (20) *Parahsuum* cf. *hiconocosta* Baumgartner et De Wever, sample A02X3/7; (21) *Parahsuum izeense* (Pessagno et Whalen), sample A02X3/1; (22) *Archicapsa pachyderma* Tan Sin Hok, sample Chir-15; (23) *Unuma echinatus* Ichikawa et Yao, sample Chir-11; (24) *Stichocapsa japonica* Yao, sample Chir-11.

then, to similarly colored lower Bathonian argillite. The northern segment is composed of clayey red-brown cherts overlain by red-brown siliceous–tuffaceous silty argillite that is replaced higher in the section by olive-gray silty argillite. The transition from siliceous to clayey rocks occurred within the middle Bajocian.

LITHOLOGIC–GENETIC CHARACTERISTICS OF ROCKS

In the southern segment of the Ussuri–Khekhtsir section, siliceous–clayey rocks are represented by *siliceous argillite*, *argillite*, and *tuffaceous argillite*.²

Siliceous argillite is olive-gray, massive, composed of fine-grained scaly quartz–chalcedony and clayey aggregates with an admixture of small ore mineral particles. They contain up to 50% radiolarian skeletons, which are replaced sometimes by yellowish green chlorite, rare fine-grained silty quartz grains, and muscovite flakes. The SiO₂ and Al₂O₃ contents in the siliceous argillite are 76.5 and approximately 11%, respectively (Table 2). According to their chemical composition, they are close to the underlying clayey cherts, although they have a lower hardness and lack a shelly fracture. The high SiO₂ content in the siliceous argillite is likely explained by the abundant radiolarian skeletons.

The *argillite* is olive-gray bedded and differs from the siliceous argillite in its lower contents of quartz–chalcedony aggregates and radiolarians (not more than 30%). The thin horizontal and flat wavy lamination is determined by the oriented arrangement of radiolarian skeletons and clayey particles. The SiO₂ and Al₂O₃ contents in the argillite are 64 and approximately 14%, respectively (Table 2).

The *tuffaceous argillite* is distinguishable owing to its yellowish brown coloration and higher content of silt-sized quartz clasts; the rock also contains plagioclase

crystals and a subordinate quantity of radiolarian skeletons.

The northern segment of the section is characterized by different siliceous–clayey rock varieties. They are *siliceous–tuffaceous silty argillite* and *silty argillite*.

The *siliceous–tuffaceous silty argillite* is a massive red-brown rock consisting of quartz–chalcedony aggregates and clay minerals with abundant disseminated hematite particles. Angular silt-sized quartz and plagioclase clasts and rock fragments composed of cryptocrystalline to fine-grained quartz with an admixture of clay minerals constitute 20–40% of the rock under consideration (Fig. 4). The clasts are probably acid pyroclastic material. The rock contains rare deformed radiolarian skeletons. It is characterized by a chaotic microstructure determined by an irregular distribution of detrital material. The relationship between the siliceous–tuffaceous silty argillite and clayey red-brown cherts of Member 1 is unknown. The clayey red-brown cherts contain, however, up to 20% silt-sized clastic material similar to that observed in the siliceous–tuffaceous silty argillite, while the basal part of the latter encloses lenses of clayey red-brown cherts. These features and the close age of the rocks imply that siliceous–tuffaceous silty argillite overlies clayey red-brown cherts. The latter are locally characterized by a lenticular–laminated microstructure owing to the oriented arrangement of clay minerals, radiolarian skeletons, and lenticular inclusions (1–2 mm thick and 3–4 mm long) with a higher SiO₂ content and more abundant radiolarians (Fig. 4). As compared with the clayey red-brown cherts, siliceous–tuffaceous silty argillite is characterized by lower SiO₂ and higher Al₂O₃ contents (Table 2).

The *silty argillite* is an olive-gray to greenish gray rock composed of clay minerals with an admixture of small ore mineral grains and carbonaceous matter. Angular fine to silt-sized quartz and rare plagioclase clasts and flakes of mica minerals constitute 30–40% of the rock. The latter is barren of radiolarians being of a clayey composition (Table 2). Sandstones that form interbeds among the silty mudstones are inequigranular, poorly sorted, and with basal cement and a graded bedding (Fig. 4). Compositionally, they correspond to feldspar–quartz graywackes with dominant acid volcanics among the clastic material (70–75%). The clasts

² The siliceous and siliceous–clayey rocks were discriminated based on their morphological features (fracture, hardness, and others) and SiO₂ contents, which were determined using the formula SiO₂ free = SiO₂ bulk – 2.4 Al₂O₃. The coefficient 2.4 is equal to the SiO₂/Al₂O₃ ratio in the clayey fraction of the chlorite–hydromicaceous composition most widespread in the siliceous and clayey rocks of Sikhote Alin [4]. In siliceous, clayey, and siliceous–clayey rocks, the SiO₂ free content is >80, 50–80, and <50%, respectively.

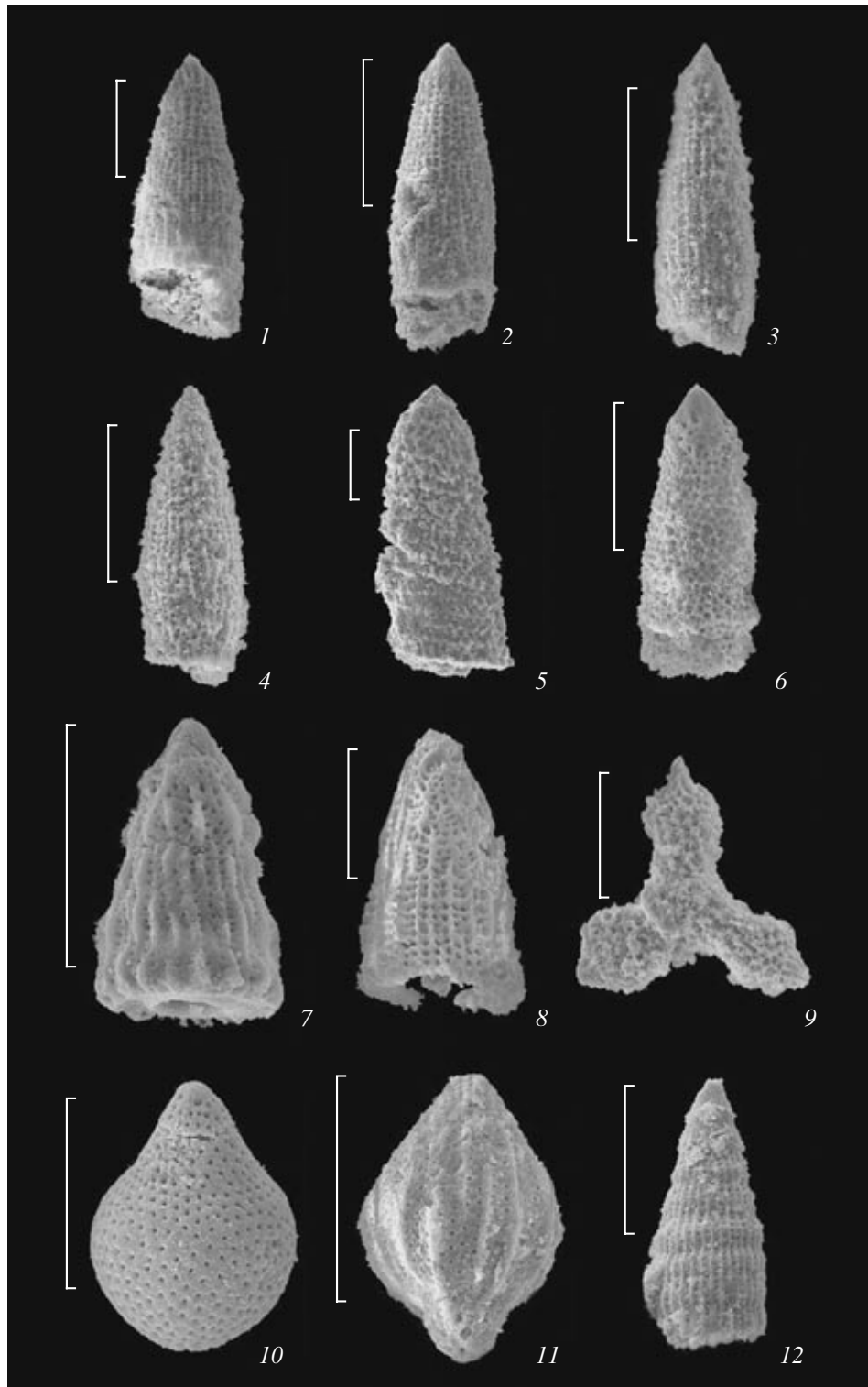


Plate 2 (Contd.)

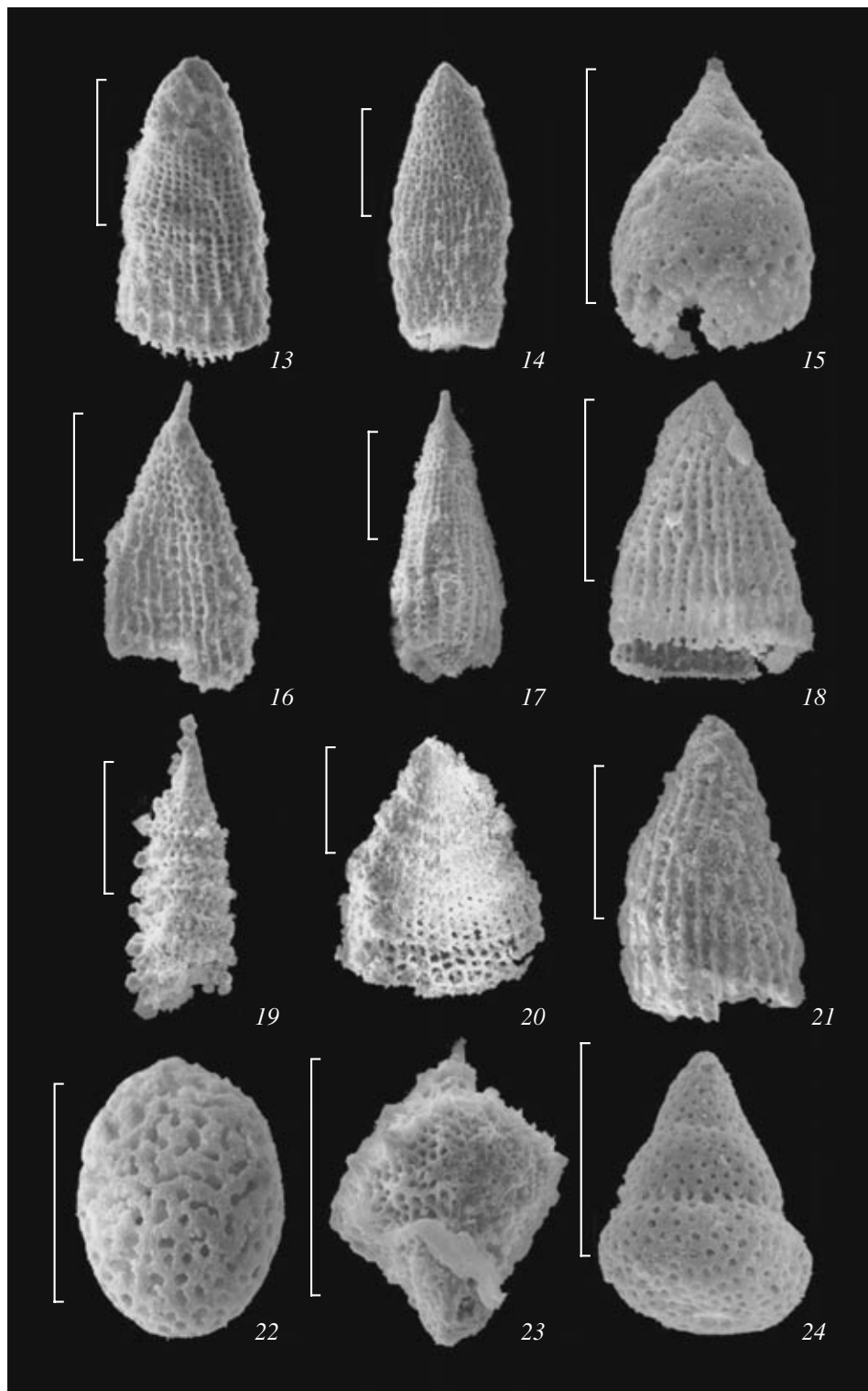


Table 3. Mineral composition (%) of the heavy fraction (0.01–0.25 mm) from some Jurassic rocks of the Ussuri–Khekhtsir section

Sample	Rock	Number of grains	Cpx	Opx	Hb	Ep	Grn	Zr	Rt	Sph	Lcx	Mt	Ilm	Chr
A02X1/3	Tuffaceous argillite	192	99.0	1.0	–	–	–	–	–	–	–	–	–	–
A02X2/2	Silty argillite	198	43.5	–	–	0.5	1.0	3.5	–	–	–	–	51.5	–
A02X3/3	Silty argillite	123	–	–	0.8	–	2.4	19.6	–	0.8	–	–	74.8	1.6
A02X3/4	Silty argillite	68	26.5	8.8	1.5	–	–	1.5	–	1.5	1.5	–	58.7	–
A02X3/7	Clayey red-brown cherts	625	1.0	0.8	0.8	1.1	2.9	16.5	0.3	–	0.6	3.8	63.1	9.1
A02X3/9	Sandstone	512	–	0.4	–	4.7	14.0	19.9	–	0.6	0.8	–	49.2	10.4

Note: (Cpx) clinopyroxene; (Opx) orthopyroxene; (Hb) hornblende; (Ep) epidote; (Grn) garnet; (Zr) zircon; (Rt) rutile; (Sph) sphene; (Lcx) leucoxene; (Mt) magnetite; (Ilm) ilmenite; (Chr) chromite; (–) not detected. Analysts V.I. Tikhonova and P.D. Gasanova.

Table 4. Chemical composition (wt %) of some heavy minerals from Middle Jurassic rocks of the Ussuri–Khekhtsir section

Sample	SiO ₂	TiO ₂	Al ₂ O ₃	Cr ₂ O ₃	FeO*	MnO	MgO	CaO	Na ₂ O	K ₂ O	Sum
Clinopyroxene											
A02X1/3	53.31	0.06	2.04	0.14	4.50	0.17	16.33	23.22	0.20	–	99.97
A02X1/3	51.98	0.25	3.14	0.08	4.95	0.08	15.19	23.47	0.20	–	99.34
A02X1/3	50.38	0.42	4.65	–	5.53	0.17	14.27	23.31	0.24	0.01	98.98
A02X3/4	48.05	0.63	6.84	0.19	8.40	0.27	12.72	23.31	0.25	–	100.66
A02X3/4	53.60	0.19	2.02	0.14	4.93	0.01	16.40	23.23	0.16	0.02	100.70
A02X3/4	53.11	0.24	2.63	0.02	4.97	0.04	15.77	23.63	0.16	0.01	100.58
Chromite											
A02X3/7	n.a.	2.50	13.13	45.50	30.55	0.09	11.97	n.a.	n.a.	n.a.	103.74
A02X3/7	n.a.	2.21	12.72	46.01	30.21	–	12.32	n.a.	n.a.	n.a.	103.47
A02X3/7	n.a.	4.21	12.93	38.42	35.66	0.13	11.98	n.a.	n.a.	n.a.	103.34
Garnet											
A02X3/7	37.10	0.11	21.23	–	29.08	2.65	1.13	7.72	0.02	0.06	99.10
A02X3/7	38.38	–	21.68	0.06	30.02	11.74	1.96	0.75	0.01	0.01	104.61
A02X3/7	39.48	0.15	21.78	0.11	25.62	3.15	3.10	9.44	0.04	0.03	102.90

Note: The (FeO*) total iron was analyzed as FeO; (–) not detected, (n.a.) not analyzed. The minerals were analyzed using a JXA-8100 microprobe at the Far East Geological Institute, Far East Division, Russian Academy of Sciences. The analyst was N.I. Ekimova.

contain quartz and plagioclase porphyric crystals and are characterized by microfelsite and microhypidioritic-granular textures. There are also granitoid fragments representing integrowths [spelling?] of large quartz and feldspar crystals and rare clasts of sedimentary and metamorphic rocks: quartz–micaceous schist, shale, siltstone, sandstone.

The siliceous and siliceous–clayey rocks in the southern and northern segments of the Ussuri–Khekhtsir section also differ in the mineral composition of the heavy fraction (Table 3). In the rocks of the southern segment, heavy minerals are rare. Only in one of the samples from Member 5, they are present in notable quantity being dominated by green clinopyroxene (99%). In the northern segment, heavy minerals occur in all the rock varieties, where they are represented by

zircon–ilmenite associations with subordinate garnet, epidote, chromite, and rare orthopyroxene, hornblende, sphene, leucoxene, and magnetite. Some samples of silty argillite are enriched in clinopyroxene. Similar associations of heavy minerals are also characteristic of sandstones that form interbeds among silty argillite.

The chemical composition of some heavy minerals allows the source rocks and the geological properties of their provenance to be determined [45]. We studied the geochemical composition of the clinopyroxene, garnet, and chromite (Table 4).

Detrital clinopyroxenes from the Ussuri–Khekhtsir section are represented by augite and salite. Their magmatic sources are determined using a discrimination diagram [38, 50]. Figure 5a shows that they are grouped near the line that divides clinopyroxenes of alkali and

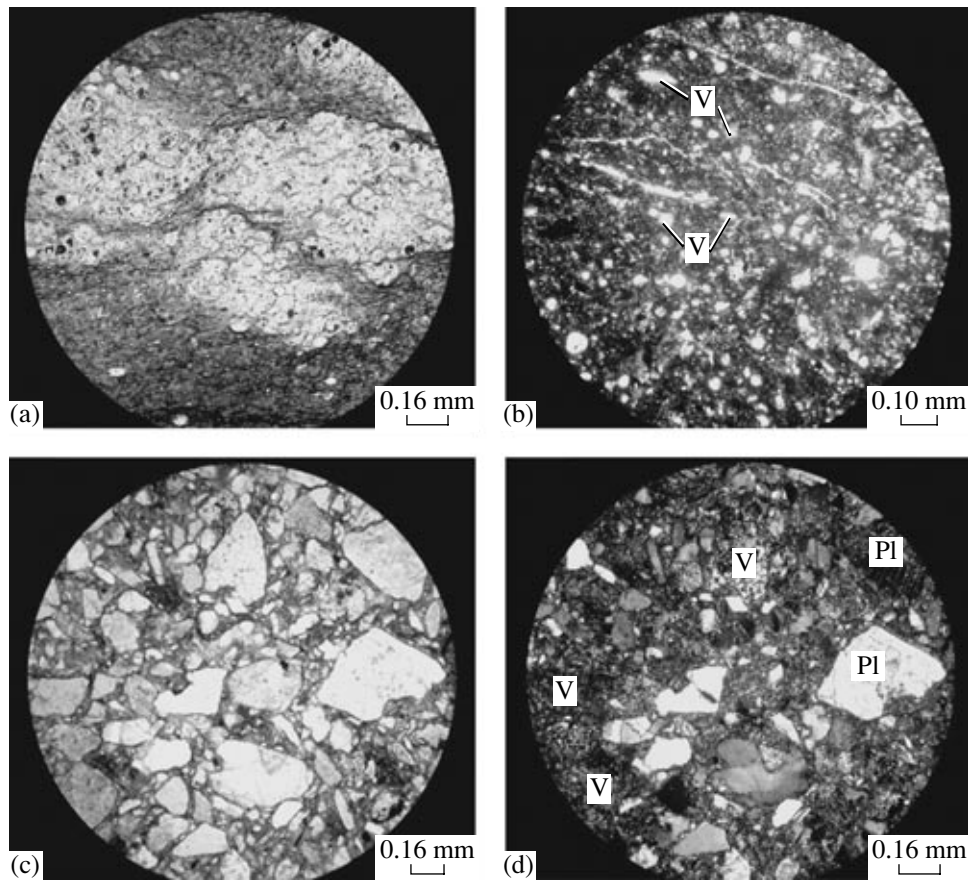


Fig. 4. Thin sections of sedimentary rocks from the Ussuri–Khekhtsir section: (a) clayey red-brown cherts from the northern segment with lenticular inclusions enriched in SiO_2 , thin section A03X3/7, parallel nicols; (b) siliceous–tuffaceous silty argillite with radiolarians and small angular clasts of acid volcanics (V) with microfelsite texture, thin section A03X3/1, parallel nicols; (c, d) fine-grained poorly sorted sandstone with basal cement. Angular clasts of plagioclase (Pl) and acid volcanics (V) with microfelsite and microhypidiomorphic–granular textures, thin section A03X3/9: (c) parallel nicols, (d) crossed nicols.

normal basalts. The low Ti and Na contents prevent one from reaching the conclusion that they originate from alkali basalts. It is evident that most of the clinopyroxenes are derived from island-arc basalts (Figs. 5b, 5c). In the Al_2O_3 – TiO_2 diagram (Fig. 6), the data points of the examined clinopyroxenes also fall into the field of island-arc clinopyroxenes from the sediments of the Philippine Sea and the Sea of Japan.

The garnets from the clayey red-brown cherts of the northern segment are represented by almandine with an insignificant content of pyrope and spessartine. They most likely originate from acid volcanics or granites (Fig. 7). The chromites in these rocks are characterized by a high TiO_2 content belonging to alkali intraplate basalts (Fig. 8).

Thus, the detrital heavy minerals contained in the siliceous–clayey rocks of the Ussuri–Khekhtsir section southern segment originate most likely from volcanics of the convergence zone. The provenance of the siliceous, siliceous–clayey, and detrital rocks from its northern segment, which contain abundant zircon, ilmenite, and garnet, is largely characterized by acid

volcanics of the continental margin with an insignificant admixture of alkali basalts of oceanic islands and island-arc volcanics.

The rocks under consideration are of a clayey composition and contain remains of planktonic microorganisms along with an insignificant admixture of silt-sized terrigenous and volcanic clastic material. These features are inherent to present-day [15] and older [2, 40] hemipelagic sediments. The olive-gray radiolarian siliceous argillite and its silica-free variety of the southern segment accumulated in relatively deep-water settings of the hemipelagic zone populated by abundant radiolarians. The thin horizontal and gentle wavy lamination in the argillite suggests low-energy hydrodynamics in the bottom layer. The low content of terrigenous clastics in these rocks and absence of heavy minerals originating from continental sources imply a significant remoteness of the sedimentation area from the continent. Only pyroclastic material was supplied intermittently to this area to form tuffaceous argillite.

The siliceous–clayey sediments of the Ussuri–Khekhtsir section northern segment accumulated in the

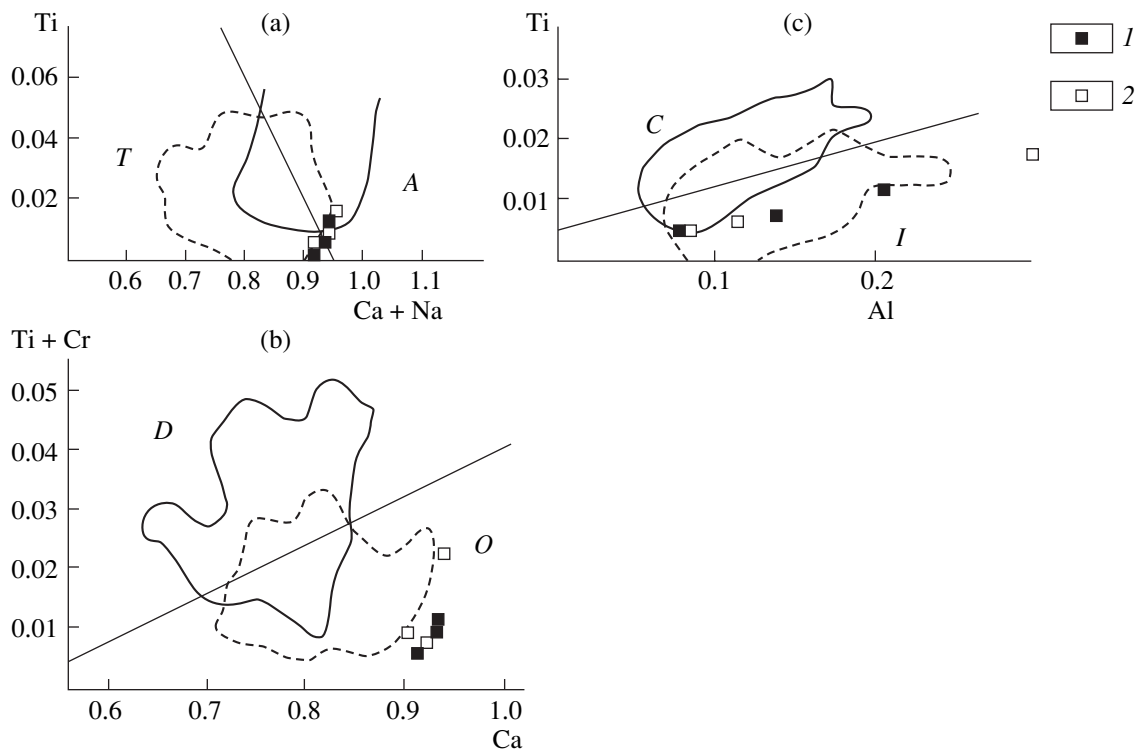


Fig. 5. Discrimination diagrams for clinopyroxenes from basalts of different tectonic settings, after [38]: (a) for clinopyroxenes from normal (*T*), alkalic intracontinental, and oceanic-island (*A*) basalts; (b) for clinopyroxenes from marginal continental, island-arc basalts (*O*) and MORB, abyssal tholeiites, and transitional riftogenic basalts (*D*); (c) for clinopyroxenes from calc-alkaline (*C*) and tholeiitic marginal continental and island-arc basalts (*I*). Values are given in f.u. (1, 2) clinopyroxenes: (1) from mudstones of the Ussuri–Khekhtsir section (southern segment), sample A02X1/3, (2) silty mudstones from the section (northern segment), sample A02X3/4.

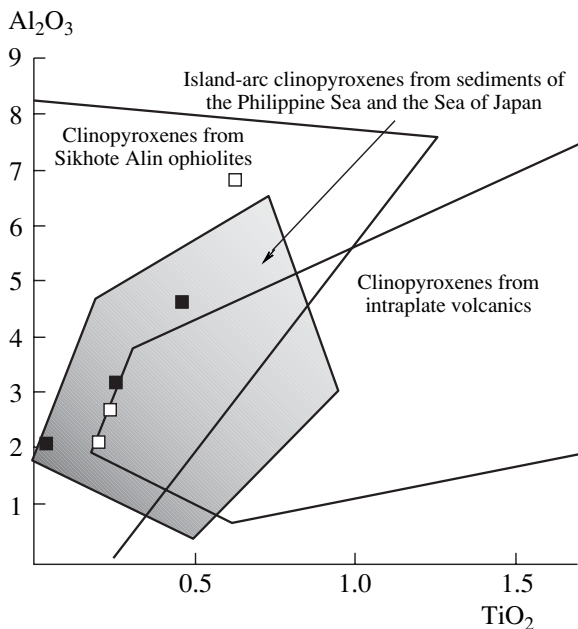


Fig. 6. Diagram of Al_2O_3 – TiO_2 for clinopyroxene from the Jurassic clayey rocks of the Ussuri–Khekhtsir section. The composition fields of clinopyroxenes from the possible source rocks are after [50]. For the legend, see Fig. 7.

other hemipelagic area of the sedimentation domain. They host the zircon–ilmenite association of heavy minerals and acid pyroclastics, which indicates the significant role of continental provenance and volcanics of the marginal continental arc in sedimentation. The presence of abundant finely dispersed hematite in the siliceous–tuffaceous silty argillite and underlying clayey red-brown cherts suggests their formation in oxidizing environments below the oxygen minimum layer. The chaotic and lenticular–laminated structure of those rocks and presence of siliceous inclusions are evidence of high-energy hydrodynamics in the bottom layer. The silty argillite accumulated in relatively calm reducing environments. The surface waters were populated by rare radiolarians or were free of them. The graded bedding and poor sorting of the clastics in sandstones forming interbeds among the silty argillite indicate an intermittent influx of terrigenous material with turbidite flows.

STRUCTURE OF THE USSURI–KHEKHTSIR SECTION AND ITS FORMATION

According to recent concepts of the accretionary prism formation [11, 20, 21, 26] and principles of tec-

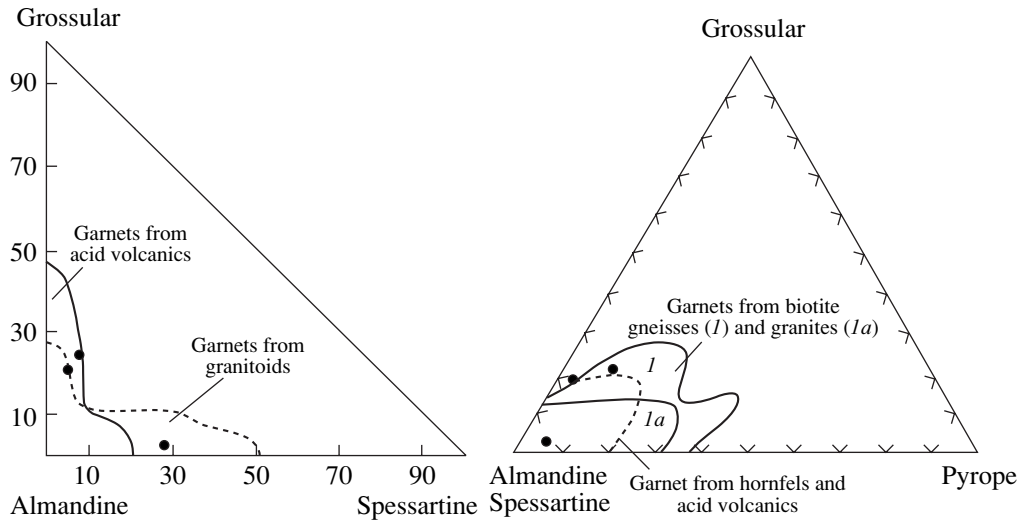


Fig. 7. Compositional diagrams for garnets from clayey red-brown cherts of the Ussuri-Khekhtsir section. The composition fields of garnets from acid igneous and metamorphic rocks are after [19].

tono-stratigraphy [31, 47], tectono-stratigraphic complexes are their main structural elements. The tectono-stratigraphic complex can be described as a lenticular or stratiform geological body representing a combination of tectonic sheets and blocks, which differ from neighboring geological bodies by the composition, age, and genesis of the constituting rocks, deformations, and metamorphic degree. This reflects a particular episode in the formation of an ancient accretionary prism, when the primary stratigraphic succession of sediments reflects the accretion age and settings, while the mode of deformations and structural particularities result from accretionary and post-accretionary tectonics. The accretion age may most accurately be determined using the youngest clastic sediments from the upper part of the primary stratigraphic succession of the complex. Indirectly, it can be derived from the age of hemipelagic sediments, which indicate approaching of the oceanic plate to the convergence zone [33, 46, 48].

The age of the clastic sediments in the Ussuri-Khekhtsir section is unknown. The difference in the composition and age of the siliceous-clayey sediments from the northern and southern segments of the section suggests that they accumulated in different areas of the hemipelagic sedimentation zone and belong to tectono-stratigraphic complexes that appeared at the initial stages of the accretionary prism formation. The earlier accretion stage is reflected in the tectonic sheets and blocks of the northern and central segments of the section. They are composed of platy cherts, dark gray silty argillite and siltstone with tuff and tuffite interbeds, pebbly mixtites, foliated and brecciated rocks, in addition to upper Aalenian-lower Bajocian clayey red-brown cherts and middle Bajocian red-brown siliceous-tuffaceous silty argillite and olive-gray silty argillite. The sheet packet is deformed into a large asymmetric synform with a gentler northwestern limb

[8]. The reconstructed initial bedding succession in this tectono-stratigraphic complex is the following (from the base upward): platy cherts and red-brown cherts, clayey red-brown cherts, siliceous-tuffaceous silty argillite, silty argillite with sandstone interbeds, silty argillite and siltstone with tuff and tuffite interbeds, and various pebbly mixtites intercalated by bedded clastic sediments. This stage was followed by accretion of fragments of the oceanic plate sedimentary cover that is now developed in the southern segment of the Ussuri-

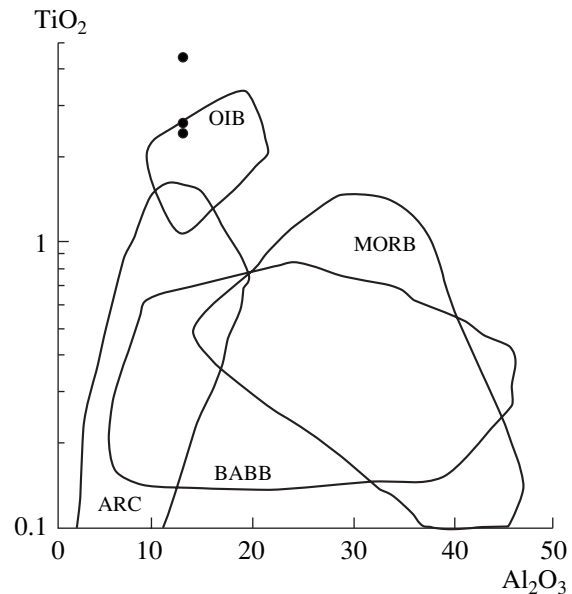


Fig. 8. Diagram of Al_2O_3 - TiO_2 for chromites from clayey red-brown cherts of the Ussuri-Khekhtsir section. The composition fields of chromites from the mid-ocean ridge (MORB), back-arc basin (BABB), oceanic island (OIB), and island arc (ARC) basalts are after [37].

Khekhtsir section. They form a packet of tectonic sheets overturned at steep angles westward. The hemipelagic sediments are represented by the Lower Bathonian olive-gray siliceous argillite and its variety barren of siliceous material. In addition, there are also upper Bajocian clayey cherts, upper Toarcian–middle Bajocian clayey red-brown cherts, older cherts and red-brown cherts, basalts, irregularly alternating silty argillite and sandstone, pebbly mixtite, and foliated and brecciated rocks.

Thus, the Ussuri–Khekhtsir section comprises two different-age tectonic-stratigraphic units differing in their composition, origin, and the deformation patterns of their hemipelagic sediments. After their correlation, in the future, with tectono-stratigraphic units in other areas of the Khabarovsk terrane, these complexes may offer the opportunity to specify its structure and formation history.

CONCLUSIONS

The lithologic–stratigraphic study of siliceous–clayey sediments outcropping in the western spurs of the Bol'shoi Khekhtsir Range on the left side of the Ussuri River (Ussuri–Khekhtsir section) revealed that they are characterized by a particular composition, age, and origin in different areas. The northern segment of the section is composed of middle Bajocian red-brown tuffaceous silty mudstones and olive-gray silty mudstones with arkose sandstone interbeds that overly upper Aalenian–middle Bajocian clayey red-brown cherts. The thickness of these sediments is 95 m. They accumulated under the influence of continental provenance and volcanism in the marginal continental arc.

The southern segment of the section consists of lower Bathonian olive-gray siliceous argillite, argillite, and yellowish brown tuffaceous argillite conformably overlying upper Bajocian greenish gray clayey cherts. The thickness of the sediments is 25 m. They accumulated far away from the continent in a relatively deep sedimentation basin with abundant radiolarians in the surface waters. The rocks under consideration accumulated in different areas of the hemipelagic zone of the past ocean and represent two tectono-stratigraphic complexes that characterize certain stages in the evolution of the Khabarovsk terrane, an element of the Jurassic accretionary prism.

ACKNOWLEDGMENTS

We are grateful to V.V. Golozubov for constructive discussion of the manuscript and T.M. Mikhailik for assistance in its preparation. This work was supported by the Russian Foundation for Basic Research (project no. 03-05-64099) and the Far East Division of the RAS (grant no. 06-III-A-08-316).

Reviewer N. Yu. Bragin

REFERENCES

1. Ch. B. Borukaev and B. A. Natal'in, "Accretionary Tectonics in the Southern Russian Far East," *Geol. Geofiz.* **35** (7–8), 89–93 (1994).
2. N. Yu. Bragin, *Radiolarians and Lower Mesozoic Sequences in the East of the USSR* (Nauka, Moscow, 1991) [in Russian].
3. N. Yu. Bragin, "Stratigraphy of the Upper Paleozoic and Mesozoic Sequences in the Khabarovsk Region," *Izv. Akad. Nauk SSSR, Ser. Geol.*, No. 9, 35–40 (1992).
4. Yu. G. Volokhin, *Silicic Rocks in the Sikhote Alin and the Origin of Geosynclinal Silicic Sequences* (Dal'nevost. Nauchn. Tsentr Akad. Nauk SSSR, Vladivostok, 1985) [in Russian].
5. *Geology of the USSR. The Khabarovsk Krai and the Amur Oblast* (Nedra, Moscow, 1966), Vol. 19, Chapt I [in Russian].
6. V. V. Golozubov, Doctoral Dissertation in Geology and Mineralogy (Moscow, 2004).
7. S. V. Zybrev and B. A. Natal'in, "Age and Tectonic Setting of Volcanogenic–Siliceous and Terrigenous Rocks in the Vicinity of Khabarovsk," in *Proceedings of the 4th Russian Far East Regional Interdepartmental Conference on the Precambrian and Phanerozoic Stratigraphy of Transbaikalia and the Southern Russian Far East* (Khabarovsk, 1990), pp. 173–175 [in Russian].
8. S. V. Zybrev, "A Stratigraphic Record of the Cherty–Terrigenous Complexes of the Khekhtsir Ridge and Kinematics of Asymmetric Folds—Indicators of Subduction Accretion," *Tikhookean. Geol.* **17** (1), 76–84 (1998).
9. I. V. Kemkin and R. A. Kemkina, "Taukha Terrane of Southern Sikhote Alin: Geology and Evolution," *Geotektonika* **34** (5), 71–79 (2000) [*Geotectonics* **34** (5), 407–427 (2000)].
10. I. V. Kemkin and A. N. Filippov, "Structure and Formation History of the Samarka Accretionary Prism," *Geotektonika* **36** (5), 79–88 (2002) [*Geotectonics* **36** (5), 412–421 (2002)].
11. I. V. Kemkin, Doctoral Dissertation in Geology and Mineralogy (Vladivostok, 2003).
12. G. L. Kirillova, "Structure of the Jurassic Accretionary Prism in the Amur Region: Aspects of Nonlinear Geodynamics," *Dokl. Akad. Nauk* **386** (4), 515–518 (2002) [*Dokl. Earth Sci.* **386** (4), 763–766 (2002)].
13. T. V. Klets, *Triassic Biostratigraphy and Conodonts of the Middle Sikhote Alin* (Novosibirsk. Univ., Novosibirsk, 1995) [in Russian].
14. M. V. Martynyuk, A. F. Vas'kin, and A. S. Vol'skii, *Geological Map of the Khabarovsk Krai and the Amur Oblast and Explanatory Note* (Khabarovsk, 1988) [in Russian].
15. I. O. Murdmaa, *Facies of Oceans* (Nauka, Moscow, 1987) [in Russian].
16. B. A. Natal'in and S. V. Zybrev, *Structure of Mesozoic Sequences in the Amur River Valley* (Guidebook for Geological Excursions) (Khabarovsk, 1989) [in Russian].
17. B. A. Natal'in, "Mesozoic Accretionary and Collisional Tectonics in the Southern Far East of the USSR," *Tikhookean. Geol.*, No. 5, 3–23 (1991).

18. A. I. Savchenko, "The Mesozoic of Northern Sikhote Alin and Lower Amur Region," *Sov. Geol.*, No. 12, 78–95 (1961).
19. V. N. Sobolev, *Genetic Types of Garnets* (Nauka, Moscow, 1964) [in Russian].
20. S. D. Sokolov, "Formation of Active Continental Margins and Vertical Accretion," in *Vertical Accretion of the Earth's Crust: Factors and Mechanisms*, Ed. by Yu. G. Leonov (Nauka, Moscow, 2002) (Tr. Geol. Inst. Ross. Akad. Nauk, Issue 542) [in Russian].
21. S. D. Sokolov, "Accretionary Tectonics: The State of the Art," *Geotektonika* **37** (1), 3–18 (2003) [*Geotectonics* **37** (1), 1–14 (2003)].
22. A. N. Filippov and I. V. Kemkin, "Kultukhinskaya Formation"—A Tectonostratigraphic Complex of a Jurassic–Berriassian Accretionary Prism in the Western Sikhote Alin, Tikhookean. Geol. **23** (4), 43–53 (2004).
23. A. I. Khanchuk, Doctoral Dissertation in Geology and Mineralogy (Moscow, 1993).
24. A. I. Khanchuk, "Formation of Ore Deposits Based on Paleogeodynamic Analysis," in *Ore Deposits of Continental Margins* (Dal'nauka, Vladivostok, 2000), pp. 5–34 [in Russian].
25. A. I. Khanchuk and I. V. Kemkin, "Mesozoic Geodynamic Evolution of the Sea of Japan Region," *Vesti Dal'nevost. Otd. Ross. Akad. Nauk*, No. 6, 94–108 (2003).
26. N. P. Chamov, "Lithogenesis of Sediments in Accretionary Prisms and Its Role in Continental Crust Formation," in *Vertical Accretion of the Earth's Crust*, Ed. by Yu. G. Leonov (Nauka, Moscow, 2002), pp. 38–55 [in Russian].
27. E. K. Shevelev, "Age of Volcanogenic–Siliceous–Terrigenous Deposits in the Basement of the Middle Amur Depression," *Tikhookean. Geol.*, No. 3, 13–16 (1987).
28. P. O. Baumgartner, L. O'Dogherty, S. Gorican, et al., "Radiolarian Catalogue and Systematic of Middle Jurassic and Early Cretaceous Tethyan Genera and Species," in *Middle Jurassic to Lower Cretaceous Radiolarians of Tethys: Occurrences, Systematic, Biochronology*, Ed. by P. O. Baumgartner et al., *Mem. Geol. Lausanne* **23**, (37–685) 1995.
29. W. H. Berger and E. L. Winterer, "Plate Stratigraphy and Fluctuating Carbonate Line," in *Pelagic Sediments on Land and under the Sea*, Ed. by K. J. Hsu and H. Jehkyns (Int. Assoc. Sediment. Spec. Publ., 1974), No. 1, pp. 11–48.
30. M. Faure and B. A. Natal'in, "The Geodynamic Evolution of the Eastern Eurasian Margin in Mesozoic Times," *Tectonophysics* **208** (4), 397–411 (1992).
31. K. J. Hsu, "Principles of Melanges and Their Bearing on the Franciscan-Knoxville Paradox," *Bull. Geol. Soc. Am.* **79** (8), 1063–1074 (1968).
32. K. Ishida, N. Ishida, T. Sakai, et al., "Radiolarians from Khabarovsk Section," in *Upper Jurassic–Cretaceous Deposits of East Asia Continental Margin along the Amur River. Field Excursion Guidebook* (Dal'nevost. Otd. Ross. Akad. Nauk, Khabarovsk, 2002), pp. 23–25 [in Russian].
33. Y. Isozaki, S. Maruyama, and F. Furuoka, "Accreted Oceanic Materials in Japan," *Tectonophysics* **181** (1/2), 179–205 (1990).
34. Y. Isozaki, "Jurassic Accretion Tectonics of Japan," *Island Arc* **6** (1), 25–51 (1997).
35. S. Kojima, K. Wakita, Y. Okamura, et al., "Mesozoic Radiolarians from the Khabarovsk Complex, Eastern USSR: Their Significance in Relation to the Mino Terrane, Central Japan," *J. Geol. Soc. Japan* **97** (7), 549–551 (1991).
36. S. Kojima and M. Kametaka, "Jurassic Accretionary Complexes in East Asia," in *Origin and Evolution of Jurassic Accretionary Complexes in Japan* (Memoirs Geol. Soc. Japan, 2000, No. 55, pp. 61–72).
37. D. Lenaz, V. S. Kamenetsky, A. J. Crawford, and F. Princivalle, "Melt Inclusions in Detrital Spinel from the SE Alps (Italy–Slovenia): A New Approach to Provenance Studies of Sedimentary Basins," *Contrib. Mineral. Petrol.* **139** (6), 748–758 (2000).
38. J. Leterrier, R. C. Maury, P. Thonon, et al., "Clinopyroxene Composition as a Method of Identification of the Magmatic Affinities of Paleovolcanic Series," *Earth Planet. Sci. Lett.* **59**, 139–154 (1982).
39. S. Maruyama and F. Furuoka, "Accreted Oceanic Materials in Japan," *Tectonophysics* **181** (1/2), 179–205 (1990).
40. T. Matsuda and Y. Isozaki, "Well-Documented Travel History of Mesozoic Pelagic Chert in Japan: from Remote Ocean to Subduction Zone," *Tectonics* **19** (2), 475–499 (1991).
41. A. Matsuoka, "Jurassic–Early Cretaceous Tectonic Evolution of the Southern Chichibu Terrane, Southwest Japan," *Palaeogeogr. Palaeoclimatol. Palaeoecol.* **96** (1–2), 71–88 (1992).
42. A. Matsuoka, "Jurassic and Early Cretaceous Radiolarians from Leg. 128, Sites 800 and 801, Western Pacific Ocean," *Proc. Ocean Drill. Prog. Sci. Res.* **129**, 203–220 (1992).
43. A. Matsuoka, "Jurassic and Lower Cretaceous Radiolarian Zonation in Japan and in the Western Pacific," *Island Arc* **4**, 140–153 (1995).
44. S. Mizutani and S. Kojima, "Mesozoic Radiolarian Biostratigraphy of Japan and Collage Tectonics along the Eastern Continental Margin of Asia," *Palaeogeogr. Palaeoclimatol. Palaeoecol.* **96** (1–2), 3–22 (1992).
45. A. C. Morton, "Geochemical Studies of Detrital Heavy Minerals and Their Application to Provenance Research," in *Developments in Sedimentary Provenance Studies*, Ed. by A. C. Morton, S. P. Todd, and P. D. W. Haughton, *Geol. Soc. Spec. Publ.*, No. 57, 31–45 (1991).
46. S. Nakae, "A Formative Process of the Sedimentary Complex of the Tamba Terrane in the Wakasa Area, Southwest Japan: An Example of Continuous Accretion," *J. Geol. Soc. Japan* **98** (6), 401–414 (1992).
47. S. Nakae, "How to Divide Accretionary Complexes: Efficiency of Tectonostratigraphy for Understanding Accretionary Tectonics," in *Origin and Evolution of Jurassic Accretionary Complexes in Japan* (Memoirs Geol. Soc. Japan, No. 55, 1–15 (2000)).
48. S. Nakae, "Regional Correlation of the Jurassic Accretionary Complex in the Inner Zone of Southwest Japan," in *Origin and Evolution of Jurassic Accretionary Complexes in Japan*, *Mem. Geol. Soc. Japan*, No. 55, 73–98 (2000).
49. B. A. Natal'in, "History and Modes of Mesozoic Accretion in Southeastern Russia," *Island Arc* **2** (1), 15–34 (1993).
50. V. P. Nechaev, A. N. Philippov, E. S. Panasenko, et al., "Heavy-Clastic Minerals in Upper Paleozoic–Lower Mesozoic Bedded Cherts of the Sikhote Alin Terranes,"

- in *Late Paleozoic and Early Mesozoic Circum-Pacific Events: Biostratigraphy, Tectonic and Ore Deposits of Primorye (Far East Russia)*, Ed. by A. Baud, I. M. Popova, J. M. Dickins, et al., Mem. Geol. Lausanne **30**, 13–24 (1997).
51. Y. Nishizono, T. Sato, and M. Murata, “A Revised Jurassic Radiolarian Zonation for the South Belt of the Chichibu Terrane, Western Kyushu, Southwest Japan,” *Mar. Micropaleontol.* **30**, 117–138 (1997).
 52. K. Sashida, Munasri, S. Adachi, and Y. Kamata, “Middle Jurassic Fauna from Rotti Island, Indonesia,” *J. Asian Earth Sci.* **17**, 561–572 (1999).
 53. A. M. Sengor and B. A. Natal’in, “Turkic-Type Orogeny and Its Role in the Marking of the Continental Crust,” *Annu. Rev. Earth Planet. Sci.* **26**, 263–337 (1996).
 54. M. Takami, R. Takemura, Y. Nishimura, and T. Kojima, “Reconstruction of Oceanic Plate Stratigraphy and Unit Division of Jurassic–Early Cretaceous Accretionary Complexes in the Okinawa Islands, Central Ryukyu Island Arc,” *J. Geol. Soc. Japan* **105** (12), 866–880 (1999).
 55. K. Wakita, S. Kojima, Y. Okamura, et al., “Triassic and Jurassic Radiolaria from the Khabarovsk Complex, Eastern Russia,” *News Osaka Micropaleontol. Spec. Vol.* **8**, 9–19 (1992).
 56. K. Wakita and I. Metcalfe, “Ocean Plate Stratigraphy in East and Southeast Asia,” *J. Asian Earth Sci.* **24** (5), 679–702 (2005).
 57. L. R. Zamoras and A. Matsuoka, “Accretion and Postaccretion Tectonics of the Calamian Island, North Palawan Block, Philippines,” *The Island Arc* **13** (4), 506–519 (2004).
 58. S. V. Zyabrev and A. Matsuoka, “Late Jurassic (Tithonian) Radiolarians from a Clastic Unit of the Khabarovsk Complex (Russian Far East): Significance for Subduction Accretion Timing and Terrane Correlation,” *The Island Arc* **8** (1), 30–37 (1999).